Proceedings of the 15th Mediterranean Conference on
Control & Automation, July 27 - 29, 2007, Athens - Greece

Sliding Mode and Adaptive Control for an Underactuated Process

E. Lucet*, Y. Liu*, N. Mechbal* and M. Vergé*
* ENSAM/LMSP, Paris, France

***Abstract*—** In this paper we design two controllers: a sliding mode controller and a new designed adaptive controller for an under actuated process with important dry friction. The two controllers are compared. Simulations and experiments are performed to evaluate the efficiency of the designed controllers.

I. INTRODUCTION

Many kinds of mechanical systems used in the industrial world are difficult to control because of the non linear model or because of the presence of the dry friction. Many friction models [1, 7] try to represent the complexity of physic phenomena. However, friction is still one of the great unknowns in mechanical systems. Besides, dry friction model is not linear [1, 2] and control of such system is quite difficult. In this work, two controllers are designed. First a sliding mode controller with varying parameter is presented. In this controller, dry friction model is not needed. Second, a multi loop adaptive controller using dry friction model is developed. Both controllers are simulated, implemented and compared.

A test bed (called MACHA) was build to analyze and to test several controllers for such a mechanical system. It consists of a cart, which is moving by the gravity on a guide rail along a sloping beam. The slope of this beam is controlled by two brushless motors with their own servo drivers (Parvex Inc.), which drive a belt mechanism mounted on the right hand side of the system. Here this system is configured with one input and one output, but the important phenomenon is the dry friction of the cart because the slope of the beam is very weak.

This paper is organized as follows.

In the second part, the plant is described and the dynamical model is given. In the third part, a non-linear sliding mode controller is designed, following the method presented in [4]. In the fourth part, an adaptive controller designed for two outputs, following the theory of [4]. A new controller is designed and is brought into application. In the fifth part simulations are presented and in the sixth part, experimental results are obtained by applying these methods to the actual process. In the conclusion, the differences between two controllers are observed.

II. DYNAMICAL MODEL

A non-linear dynamic model of the 2-link machine (see fig. 1) is established using notations of fig. 2. The linear position of the cart $x(t)$ on the beam is the underactuated joint and the angular position $\theta(t)$ of the beam is the actuated joint as it is shown in figure 2 where plan X0, Y0 is vertical. Here the bell elasticity is neglected and the motor is controlled thanks to torque reference so that the input is proportional to F_2. Two magnetostrictive sensors are used to give cart position and B position, thus beam slope $\theta(t)$ is known.

Figure 1. Process MACHA

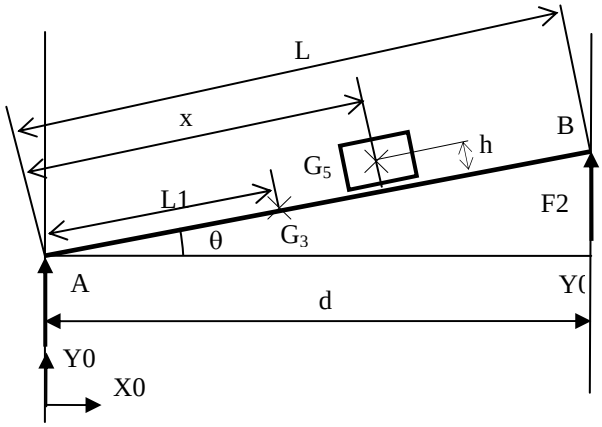

Figure 2. Notations

TABLE 1. Some values

Description		Value
Distance between the cart centre of mass G5 and the beam.	h	0.10 m
Distance between A and B.	d	1.44 m
Acceleration of gravity.	g	9.81m/s²
Overall length of the tilted beam.	L	2.20 m
Distance between point A and the beam centre of mass: G3.	L1	0.72 m
Mass of the beam.	M3	18.00 kg
Mass of the cart.	M5	2.86 kg
Inertia of the beam.	J	29.04 kg.m²

Dynamical model of this system is obtained using Lagrange equations or bond graph method [11]. This model is written in joint space as:

$$D(\underline{q})\cdot\ddot{\underline{q}}+C(\underline{q},\dot{\underline{q}})\cdot\dot{\underline{q}}+\underline{g}(\underline{q})+F(\dot{\underline{q}})\cdot\dot{\underline{q}}=\underline{u}(\underline{q}). \quad (1)$$

Where the inertial matrix is:

$$D(\underline{q})=\begin{pmatrix} M_5 & -M_5\cdot h \\ -M_5\cdot h & M_5\cdot(x^2+h^2)+J \end{pmatrix}. \quad (2)$$

The Coriolis matrix is:

$$C(\underline{q},\dot{\underline{q}})\cdot\dot{\underline{q}}=\begin{pmatrix} 0 & -M_5\cdot\dot{\theta}\cdot x \\ 2\cdot x\cdot M_5\cdot\dot{\theta} & 0 \end{pmatrix}\cdot\dot{\underline{q}}. \quad (3)$$

Gravitational torques vector is given by:

$$\underline{g}(\underline{q})=g\cdot\begin{pmatrix} M_5\cdot sin\theta \\ M_5\cdot x\cdot cos\theta - M_5\cdot h\cdot sin\theta + M_3\cdot L1\cdot cos\theta \end{pmatrix}. \quad (4)$$

Here, the vector degree of freedom is:

$$\underline{q}=\begin{pmatrix} x \\ \theta \end{pmatrix}. \quad (5)$$

In this plant, the input vector is: $\underline{u}=(0 \quad \tau_a)^T$, with F_2 the force applied by the motor and: $\tau_a=d\cdot F_2\cdot cos\theta$.

Dry friction forces are noted $F(\dot{\underline{q}})$. Here we only consider friction in joint A and friction between the cart and the beam. So we have:

$$F(\dot{\underline{q}})=\begin{pmatrix} F_{df}(\dot{x}) \\ F_{df}(\dot{\theta}) \end{pmatrix}. \quad (6)$$

Many dry friction models have been already developed; some models are static such as classical models, the Karnopp model [6], the Armstrong's model [7] etc. in these models, the friction is only a function of velocity. Some are dynamic models such as the Dahl model [8] or the LuGre model [9]. In these models, the friction is not only function of velocity but also depends on the acceleration. In our case, beam velocity and cart velocity are very small, so we use the following common classical model [10] to represent dry friction force:

$$F_{df}(\dot{u})=f_c\cdot sgn(\dot{u})+(f_S-f_c)\cdot e^{-|\dot{u}|^{C_S}}\cdot sgn(\dot{u})+f_v\cdot\dot{u}. \quad (7)$$

f_c, f_s, f_v and C_s are four positive constants to define for degree of freedom, and $sgn(\dot{u})$ stand for the sign of the velocity of $u(t)$. f_c is called coulomb coefficient, f_s is the stiction coefficient and f_v is the viscous coefficient. Numerical values of these coefficients have been identified using genetic algorithms [5]. In part IV this model is written in the form: $F(\dot{x})=\underline{S}^T(\dot{x})\cdot\underline{P}$, where:

$$\underline{S}^T(\dot{x})=[e^{-\left|\frac{\dot{x}}{\dot{x}_s}\right|^{\delta_s}}sgn(\dot{x}),\ (1-e^{-\left|\frac{\dot{x}}{\dot{x}_s}\right|^{\delta_s}}sgn(\dot{x}))\cdot sgn(\dot{x}),\dot{x}]. \quad (8)$$

And: $\underline{P}=(f_s,f_c,f_v)^T$ is a vector collecting dry friction parameters.

III. Design of Sliding Mode Controller

The goal of the controller is to move the cart from one position to another position, trying to reduce static error. Physical limits of the variables have to be taken into account. To design the sliding mode controller dry friction is neglected so only viscous friction is considered. Thus, friction matrix becomes:

$$F=\begin{pmatrix} f_{v\_c} & 0 \\ 0 & f_{v\_b} \end{pmatrix}. \quad (9)$$

Where: f_{v_c}, f_{v_b}, are positive, constant and represent viscous friction. Equation (1) can be partitioned as:

$$D(\underline{q})\cdot\begin{pmatrix} \ddot{x} \\ \ddot{\theta} \end{pmatrix}+\begin{pmatrix} F_p \\ F_a \end{pmatrix}=\begin{pmatrix} 0 \\ \tau_a \end{pmatrix}. \quad (10)$$

Where:

$$\begin{pmatrix} F_p \\ F_a \end{pmatrix}=C(\underline{q},\dot{\underline{q}})\cdot\dot{\underline{q}}+\underline{g}(\underline{q})+F\cdot\dot{\underline{q}}$$
$$=\begin{pmatrix} -M_5\cdot\dot{\theta}^2+M_5\cdot g\cdot s\theta+f_{v\_c}\cdot\dot{x} \\ 2M_5\cdot x\cdot\dot{x}\cdot\dot{\theta}+M_5\cdot g(x\cdot c\theta-h\cdot s\theta)+M_3\cdot g\cdot L_1\cdot c\theta+f_{v\_b}\cdot\dot{\theta} \end{pmatrix} \quad (11)$$

Developing equation (10) one can obtain for each degree of freedom:

$$\ddot{\theta}=\frac{M_5\cdot h\cdot\ddot{x}-F_a+\tau_a}{M_5\cdot(x^2+h^2)+J} \quad (12)$$

$$\ddot{x}=h\cdot\ddot{\theta}-\frac{F_p}{M_5} \quad (13)$$

In order to manage the cart position, the sliding mode controller has to control its acceleration $\ddot{x}(t)$. Consequently, the term $\ddot{x}(t)$ must be isolated. Substituting (12) in (13) we obtain:

$$\ddot{x}=D\tau\cdot\tau_a+H_p. \quad (14)$$

Where:

$$D_\tau=\frac{h}{M_5\cdot x^2+J} \quad (15)$$

$$H_p=\frac{-h\cdot M_5\cdot F_a-(M_5(x^2+h^2)+J)\cdot F_p}{(M_5\cdot x^2+J)\cdot M_5} \quad (16)$$

The sliding mode controller is defined as:

$$\tau_a = \frac{1}{D_\tau}\cdot\left(W_{pr} - H_2\right) \tag{17}$$

Note that (17) is similar to the controller presented in [4], the difference resides in the definition of H_2. Here we have:

$$H_2 = \frac{-h\cdot M_5\cdot F_a + \left(M_5\left(x^2+h^2\right)+J\right)\cdot F_p}{\left(M_5\cdot x^2 + J\right)\cdot M_5} \tag{18}$$

Applying (17) to (14) we obtain:

$$\ddot{x} = \left(W_{pr} - H_2\right) + H_p = W_{pr} - \frac{2\cdot\left(M_5\left(x^2+h^2\right)+J\right)\cdot F_p}{\left(M_5\cdot x^2 + J\right)\cdot M_5} \tag{19}$$

This controller is separated in two parts:

$$\ddot{x} = W + \Delta W - \frac{2\cdot\left(M_5\left(x^2+h^2\right)+J\right)\cdot F_p}{\left(M_5\cdot x^2 + J\right)\cdot M_5} \tag{20}$$

Where the first part W is the nominal controller and the second part ΔW is called the robust control term. Tracking error is given by $\varepsilon = x_d - x$ where $\underline{x}_d$ is the desired position of the cart.

The sliding surface is given by $s = \dot{\varepsilon} + \lambda\cdot\varepsilon$ where λ is a positive constant. The nominal controller term is chosen as:

$$W = \ddot{x}_d + K_d\cdot\dot{\varepsilon} + K_p\cdot\varepsilon \tag{21}$$

Where K_d and K_p are two positive constants that define the settling time and the overshoot of the closed loop system. Robust controller term is a sliding mode controller and is defined as:

$$\Delta W = \frac{\rho}{\|s\| + \alpha}\cdot s \tag{22}$$

Where ρ and α are two positive constants. Parameter ρ must be rather large to allow the stability of the controller and so that α allows limiting the chattering phenomena. Using Lyapounov method, it can be proved that this controller is globally exponentially stable.

The desired position of the cart and its derivatives $x_d(t)$, $\dot{x}_d(t)$, $\ddot{x}_d(t)$ are to be chosen to define the trajectory of the cart.

IV. Design of an Adaptive Controller

In sliding mode controller, the dry friction is not taken in account, which could bring some static errors. In the design of the adaptive controller, the dry friction is considered as one part of the controller.

In the existing theories such as [4], adaptive controller is mostly SISO (single input single output) systems. But the system MACHA, has one input (force F2) and two outputs ($\theta(t)$ and $x(t)$). Thus the controller is structured in two parts. The first (Cont_c) contains the compensation of friction in point A, and the second (Cont_b) contains the compensation of friction between the beam and the cart: see fig 3.

The goal is to control the cart position, so the first part which controls the position gives the reference to the second part.

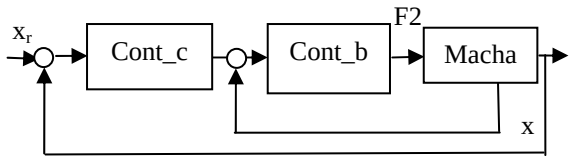

Figure 3. Two controllers

The height of the beam at the point B is $y = d\cos(\theta)$. Let $e = y - y_d$ the error. Then we obtain: $\dot{y}_r = \dot{y}_d - \lambda\cdot e$. The dynamic error is defined by: $r = \dot{e} + \lambda\cdot e$. The internal part (Cont_b) of the adaptive controller is then given as:

$$\begin{aligned} F_2\cdot d = {} & \frac{J}{d}\cdot\ddot{y}_r - k_{1b}\cdot r + \hat{F}_{fric\_b}\cdot d \\ & + M_3\cdot g\cdot L_1 - k_{ib}\cdot\int_0^t r\cdot d\tau - u_{rb} + M_5\cdot g\cdot x \end{aligned} \tag{23}$$

References $y_d(t)$, $\dot{y}_d(t)$, $\ddot{y}_d(t)$, are to be selected to define the trajectory of the cart. Parameters λ, k_{1b}, k_{ib} have to be chosen to define the closed loop performances. u_{rb} represents the system uncertainty: we have chosen, $u_{rb} = k_{2b}\cdot sgn(r)$ where k_{2b} is a constant greater than 1. $\hat{F}_{fric\_b} = \underline{S}^T(\dot{y})\cdot\underline{P}$ is used to compensate the friction.

Parameter $\underline{P}$, describing the dry friction of friction, is adapted by a positive diagonal matrix Γ_b using:

$$\dot{\underline{\hat{P}}} = \Gamma_b\cdot\underline{S^T}\cdot r \tag{24}$$

This is the adaptive part of this controller. For the cart, the controller is obtained by a similar way:

$$\begin{aligned} \frac{M_5\cdot g}{d}y_d = {} & k_{1c}\cdot r - M_5\cdot\ddot{x}_r - S^T(\dot{x})\cdot\hat{P} \\ & + k_{ic}\int_0^t r\cdot d\tau + k_{2c}\cdot\mathrm{sgn}(r) \end{aligned} \tag{25}$$

Using Lyapounov method, it has been shown [4] that this controller is globally exponentially stable.

V. Simulations

Simulations are conducted with the dynamics model elaborated in part II including the dry friction. The sampling time is chosen as Ts=10 ms and ODE 45 (Matlab) method is used to simulate the two controllers. In order to apply the reference $x_d(t)$ gradually we chose a step function filtered by first order filter of time-constant 1.5 s.

For the sliding mode controller, the parameters are chosen as: $K_p = 5\,s^{-2}$, $K_d = 0.1 s^{-1}$, $\lambda = 10\,s^{-1}$, $\rho = 0.52$ and $\alpha = 0.5$. Initial cart position is the middle of the beam, which is horizontal. Initial cart velocity and initial angular velocity of the beam are zero. The cart has to move 0.8 m towards the right. During this evolution, force input F2 has to be less than 350 N. Because the cart is not actuated, the desired position can be reached by successive rotational movements of the beam.

In fig 4, time evolution of the cart position and the reference are displayed. An excellent position tracking can be observed. The invisible static error (3 mm) remains insignificant. So that the cart reaches its desired position, the beam must have the appropriate behavior. Fig 5 shows beam rotations. A maximum value of 0.17 rad is acceptable because the limit was fixed at 0.5 rad. When the cart is in the final desired position, the beam returns to its initial horizontal position. Time evolution of the exerted force (F2) by the drive mechanism is displayed in fig 6. This force compensates the weight of the beam and the changing moment of the cart, caused by its changing position and also generates the desired movement of the beam. It reaches a maximum value of 200 N allowing the maximal angular displacement of the beam.

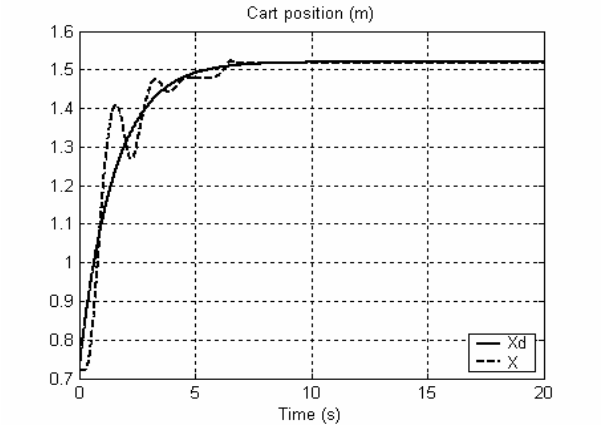

Figure 4. Simulation of the cart behavior (Sliding mode)

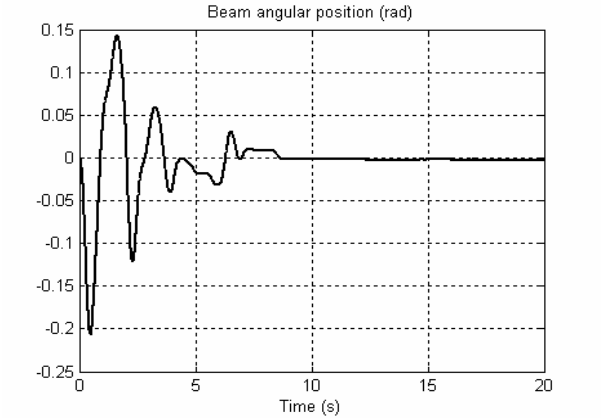

Figure 5. Simulation of the beam angle (Sliding mode)

For the adaptive controller (23, 25), the parameters selected are given as follow:

For the beam: $k_{1b} = 480$, $k_{ib} = 0$, $k_{2b} = 2$, $\lambda = 10$

For the cart: $k_{1c} = 2$, $k_{ic} = 0$, $k_{2c} = 0.1$, $\lambda = 0.1$

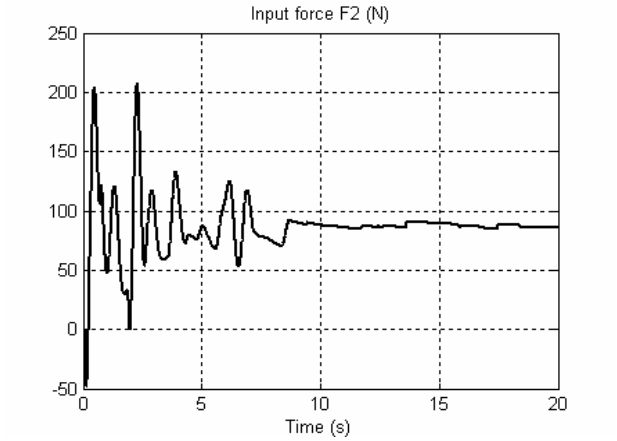

Figure 6. Simulation of the input force (Sliding mode)

And: $\Gamma_{beam} = \begin{bmatrix} 0.1 & 0 & 0 \\ 0 & 0.1 & 0 \\ 0 & 0 & 0.2 \end{bmatrix}$, $\Gamma_{cart} = \begin{bmatrix} 0.1 & 0 & 0 \\ 0 & 0.1 & 0 \\ 0 & 0 & 0.1 \end{bmatrix}$

Because the adaptive controller needs varying commands to achieve the process of adaptation. The input for this controller is different from the sliding mode controller.

Fig 7 shows input output variables using two adaptive controllers. We observe an excellent position tracking both in cart position and in beam position with zero static error.

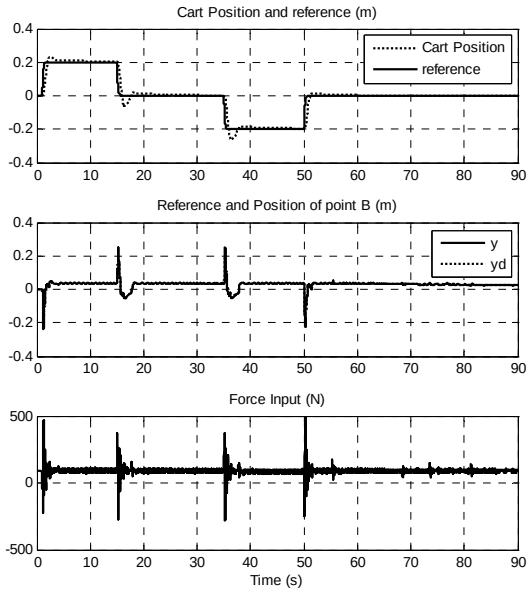

Figure 7. Simulation of the cart behavior (Adaptive)

VI. EXPERIMENTS

The experiment for the sliding mode controller is conducted with the initial cart position x_ini = 0.22 m, and with the reference step of magnitude 1 m.

In fig 8 the cart trajectory is displayed. A static error of 0.015 m is observed after 35 s, which also corresponds to fig 9, where the beam is near the horizontal position. In fact the cart does not move anymore because of the static

friction, which is a significant problem for little movements.

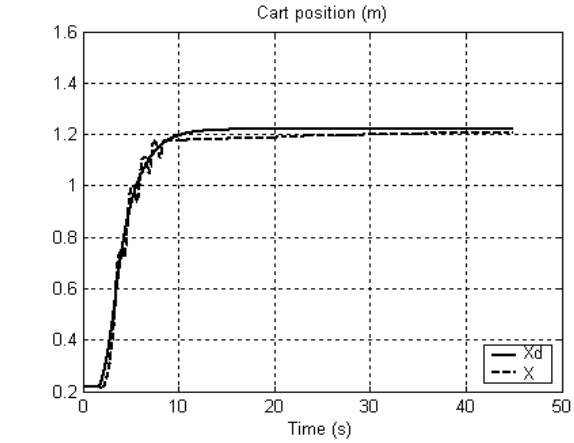

Figure 8. Cart position (Sliding)

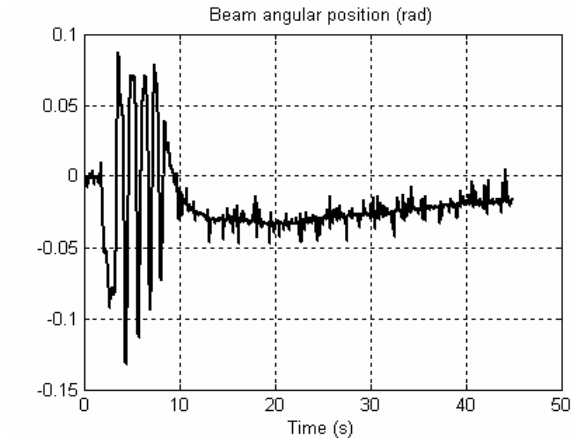

Figure 9. Beam angle (Sliding)

Figure 9 shows the chattering phenomena which is important when the cart is stuck on the beam. To reduce steady state error, we can increase the value of ρ, which increases the value of ΔW (the robust control input term). But, increasing ρ, the chattering phenomena increases and the process could present non acceptable vibrations. Notice that this controller is quite robust because we know that dry friction is not constant and that some phenomena (like elasticity of belt for example) is not taken into account. To improve the performances, a variable parameter ρ has been experimented. Here we use:

$$\rho = \rho_{max} - \left(a1 \cdot \|\dot{q}\|^2 + a2 \cdot \|\dot{\varepsilon}\| + a3 \cdot \|\varepsilon\|\right) \qquad (26)$$

When the cart is near the reference position, the value of ρ is ρ_{max}=0.78 and the value of ρ is decreasing when the cart moves away from the middle of the beam. Note: ρ is always positive, thus stability is not modified.

In fig 10, the reference step of magnitude 1 m is applied with initial position 0.22m. As we can see, final value is improved: static error is less than 0.005 m and beam rotations are quite acceptable.

In fig 11, an impulse disturbance is applied at time t=5s, when the cart is in the middle of the beam. The controller tries to stabilize the cart in the initial position. Thus, the beam rotates many times and after 10 s the cart reaches the initial position. At time t = 37 s, an opposite impulse is applied and the same conclusions can be done.

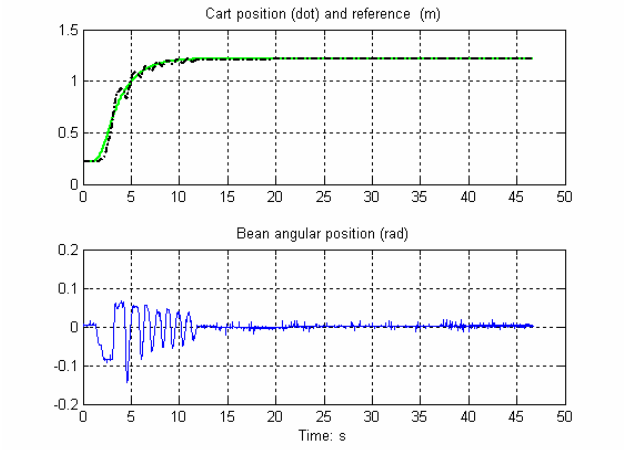

Figure 10. Step response with variation of ρ (Sliding)

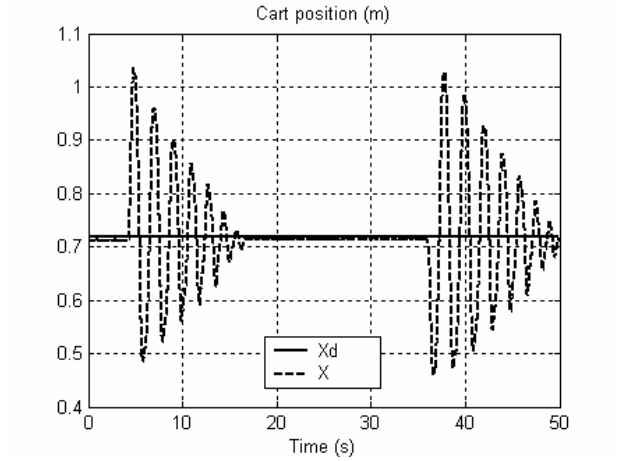

Figure 11. Disturbance rejection (Sliding)

Adaptive controller experiment is based on the hypothesis that the adaptation efficiency depends on the frequency of control modification. So the experiment is done by modify the input process every 5-10 seconds. The modification is done in the real time with an interface realized with carte dSPACE .

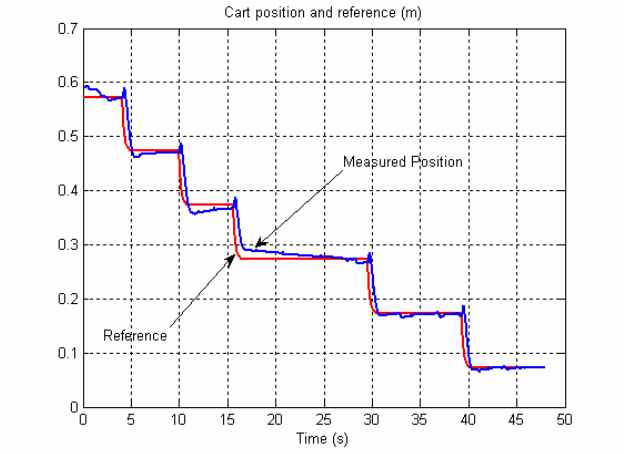

Figure 12. Cart position (Adaptive)

In fig 12 the trajectory of the cart is displayed. The cart position follows the reference position very quickly and without steady state error. Vibrations could be observed. This would be due to the sensitivity of the adaptation and to the presence of noise on the sensors.

In fig 13, the trajectory of beam is displayed, great vibration is observed, but this does not exceed the limit of the beam. In this figure, position of point B (beam extremity) and reference of this position are displayed. Here, the noise is more important and the extremity B is moving up and down very quickly. It's a little difficult to select the two Γ matrices which are very sensitive of noise.

Fig. 14 gives the evolution of stiction coefficient (fs) for the dry friction relative to the cart moving on the beam. The coefficient is nearly constant but is the most influent to the steady state error of the cart position (fig 12).

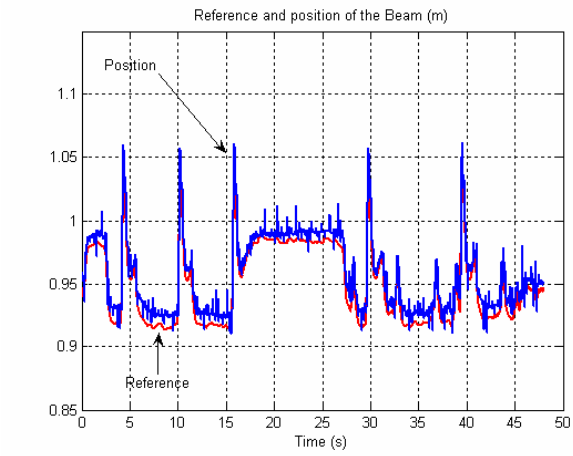

Figure 13. Beam angle (Adaptive)

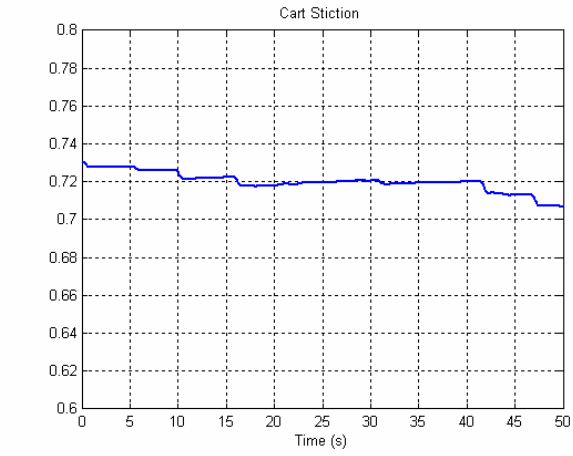

Figure 14. Stiction coefficient for the cart (Adaptive)

In conclusion, this controller has good performances because it could compensate the friction; the static error is null. Vibration is observed due to output noise.

VII. Conclusion

Control of an under actuated machine is the source of many difficulties. A sliding mode controller and an adaptive controller have to be designed and implemented on the plant. The experimental results of sliding mode controller obtained on the actual plant are very near to the results generated by simulation. This means that the model was quite reliable. Steady state error is due to static friction and friction appears to be more complicated than the way it was modeled. The static error can be reduced by modifying the sliding control parameters but the risk is to observe very important vibrations. A compromise has to be made.

An adaptive controller with the compensation of dry friction has a zero steady state error both in simulation and experiment. This means an adaptive controller is more reliable in the important dry friction case. However, the choice of Γ matrices is very difficult and many simulations and experiments have to be done. One advantage of this controller is that we can use it to detect dry friction modifications: it is a way to detect faults on this process.

This work could be extended to the whole system in which point A is moving up and down. In this case, the system has two inputs and the controller is more complex.

Another work to do is to use a dynamic model of dry friction and to use it to make fault detection.

References

[1] C.Canudas de Witt. and P. Lischinsky, "A new model for control of systems with friction." *IEEE Transaction on Automatic Control*, vol 40, pp. 419-425, 1997.

[2] H. Olsson, K. Astrom, and C. Canudas de Wit, M. Gäfvert and P. Lischinsky, "Frictions Models and Friction Compensation." *European Journal of Control*, vol 4, pp. 176-195, 1998.

[3] W. Kim, J. H. Shin and J. J. Lee, "Sliding Mode Control for a Robot Manipulator with Passive Joints," *ICASE : The Institute of Control, Automation and Systems Engineers, KOREA*, vol. 4, no. 1, March 2002.

[4] J.WANG, S.S.Ge, and T.H.Lee. *Adaptive friction compensation for servo mechanisms, Adaptive Control of Nonsmooth Dynamic Systems.* Edited by G.Tao and F.Lewis. Springer Verlag, 2001.

[5] M. Vergé, "Friction identification with genetic algorithms." IFAC World Congress Praha, 2005.

[6] D. Karnopp. Computer simulation of slip-stick friction in mechanical dynamic systems. Journal of Dynamic Systems, Measurement, and Control, 107(1): pp 100–103, 1985.

[7] B. Armstrong-Hélouvry, P. Dupont, et C. Canudas de Wit, "A survey of models, analysis tools and compensation methods for the control of machines with friction". Automatica, 30(7): pp 1083–1138, 1994

[8] P. Dahl. "A solid friction model", Technical Report TOR-0158H3107–18I-1, The Aerospace Corporation, El Segundo, CA, 1968.

[9] C. Canudas de Wit, Henrik Olsson, Karl Johan Åström, and P. Lischinsky. "Dynamic friction models and control design", Proceedings of the 1993 American Control Conference, pp 1920–1926, San Francisco (USA), 1993.

[10] R. Stribeck. "Die wesentlichen Eigenschaften der Gleit- und Rollenlager – The key qualities of sliding and roller bearings", Zeitschrift des Vereines Seutscher Ingenieure, 46(38,39): pp 1342–48, 1432–37, 1902.

[11] M. Vergé. "Modélisation pour l'ingénieur, approche par Bond Graph", Congrès Européen des Sciences et des Systèmes, Paris, Septembre 2005.